Bioprinting of novel ECM-based electroconductive hydrogels for tissue engineering

Catarina Ferreira

Instituto Superior Técnico, Lisboa, Portugal

November 2021

In this work, a novel electroconductive ECM-based bioink is formulated. Addition of the conductive polymer poly(3,4-ethylenedioxythiophene):poly(styrene sulfonate) (PEDOT:PSS), in various concentrations, in digested ECM (sisECM) preparation, led to bioinks with suitable rheological properties and improved electrical conductivity, in accordance with values found in literature. Freeform reversible embedding of suspended hydrogels (FRESH) extrusion bioprinting was used to obtain conductive sisECM scaffolds. Bioink printability was evaluated with successful results. Biocompatibility was assessed with cell seeding assays for mouse fibroblasts, with > 96.5% cell viability, and cardiomyocytes derived from human induced pluripotent stem cells, with acceptable cell adhesion on PEDOT:PSS hydrogels. Finally, fibroblasts were bioprinted on the developed bioinks, with great success in cell viability, > 93%, but some inability to maintain scaffold self-support after gelatin removal due to limitations with printing conditions.

Keywords: 3D FRESH Bioprinting, extracellular matrix, electroconductive hydrogels, cardiac tissue engineering

INTRODUCTION

Tissue engineering (TE) is an interdisciplinary field where principles of life sciences are applied to materials engineering to restore, maintain, and enhance tissue function, and has become the main process involved in cell growth and reconstruction of organs[1]. In physiological conditions, cells are organized in a complex three-dimensional (3D) microenvironment that allows the interaction between different cell types and between the cells and the extracellular matrix (ECM). TE allows the production of 3D models that can better mimic the in vivo tissue and organ conditions, using a wide variety of cells, biomaterials, growth factors and other supporting components to create functional constructs.

3D Bioprinting: 3D bioprinting has emerged as a TE method for producing tissue scaffolds to bridge the divergence between artificially engineered tissue constructs and native tissues[2,3]. Comparing with traditional methods, 3D bioprinting allows for the direct deposition of biomaterials that are encapsulated with cells or loaded with cells afterwards, in micrometer scale to form structures comparable to native tissue, such as patient-derived organs, structures for the creation of disease models and cytotoxicity detection platforms for drug and cosmetic testing, as well as for personalized medicine, where pharmaceuticals could be tested in bioprinted patient specific tissue. This allows the reduction risk of organ-rejection, elimination of preclinical animal testing, and the creation of disease models that better recapitulate the complexity of human metabolism[14].

Bioprinting techniques include extrusion bioprinting, inkjet bioprinting, laser-assisted bioprinting, and stereolithography, where bioprinting of several tissues and constructs has been successful[3-11]. Extrusion bioprinters are compatible with multiple materials with an extensive range of viscosities (30 – $6x10^7$ mPa.s) and bioinks with high cell densities (>10^8 cells/mL)[12]. The resolution of this technique is in the order of 200–1000 µm and careful control over shear stress is required to minimize cell death. Printing with low viscosity materials is challenging in traditional extrusion bioprinting because the materials need to be relatively viscous, otherwise, the bioprinted structures will have a low print resolution or even 3D self-standing structures will not be possible to print. While current 3D printing techniques can produce full-size adult organ models, the materials used generally do not mimic the mechanical properties of native tissue[13]. To address this challenge, freeform reversible embedding of suspended hydrogels, also known as the FRESH method, was developed.

FRESH extrusion bioprinting: The main difference with conventional extrusion bioprinting is that materials are extruded inside a thermo reversible gelatin-slurry microparticle support bath, used as a sacrificial material. This support bath maintains the shape of the structures until they have gelated/crosslinked and can support multiple independent crosslinking strategies, such as pH changes, divalent cations, and UV, to gel different hydrogels and other soft polymeric materials. At the end of the printing process, the sacrificial material is removed. The printing of several scaffolds for tissue engineering has been successful [14-16].

Bioinks for FRESH extrusion bioprinting: For bioprinting, the bioinks should have good printability, biocompatibility and ideal structural and mechanical properties. The materials that most closely fulfill these characteristics are hydrogels, 3D networks formed by molecular chains embedded in a water-rich environment, formed using several crosslinking mechanisms. They show tunable physicochemical properties and high biomimicry of the native tissues' ECM, and allow cell encapsulation in a highly hydrated, mechanically supportive 3D environment similar to that in many natural tissues[17]. In addition, hydrogels can be further modified with chemically and biologically active

recognition cues such as stimuli-responsive molecules and growth factors (GFs) that enhance their biofunctionality. The polymers for hydrogels can be classified into natural and synthetic polymers. Natural polymers include alginate, chitosan, hyaluronic acid, gelatin, fibrin, silk and many others, whilst the synthetic polymers include materials such as polyacrylamide (PAAm), polyvinyl alcohol (PVA), polyethylene glycol (PEG), polylactic acid (PLA), and others[18]. Bioactivity, biocompatibility, 3D geometry, antigenicity, non-toxic byproducts of biodegradation, and intrinsic structural resemblance are the most important properties of natural polymers, but their lack of mechanical strength is a major disadvantage. On the other hand, synthetic polymers are characterized by their tunable properties, endless forms, and established structures over natural polymers and their polymerization, interlinkage, and functionality of their molecular weight, molecular structure, physical and chemical features make them easily synthesized as compared to naturally occurring polymers. Depending on the cell type and application, careful selection of the materials is required.

The extracellular matrix (ECM) appears as a great candidate for a biomaterial in tissue engineering applications, and decellularized extracellular matrix (dECM) is used as it can recapitulate all the features of natural ECM. The resulting bioink is a rich medium with native growth and differentiation factors, which supports the specific functioning of the chosen cell type. In terms of dECM printability, dECM bioinks have a low viscosity[19] and because they are usually softer than most hydrogels, they need to be either mixed with other crosslinking agents to make them printable in extrusion bioprinting or printed along biocompatible thermoplastics (such as polycaprolactone) for a mechanically strong scaffold[20].

Increased Hydrogel Functionality: There is an increased demand for smart and stimuli-responsive materials to provide additional control over the material's properties and cell fate. Therefore, strategies to increase the functionality of the hydrogels will be key to achieve this. This can be done by incorporation into the hydrogel structure of nano- and microfillers with electrical, piezoelectrical and magnetic properties. For applications in the engineering of electrogenic tissues such as cardiac, neural and muscle tissues, conductivity plays an important role in mimicking the electrical conditions of in vivo tissues and can be determinant towards differentiation and functionality. Conductivity of hydrogels can be increased by addition of metal nanoparticles (NPs), carbon-based materials, and conductive polymers. PEDOT in combination with polystyrene sulfonate (PSS) (PEDOT:PSS) shows strong potential in tissue engineering due to its high stability and high electrical conductivity (1–10 S/cm), hence tuning the conducting nature of PEDOT:PSS based hydrogels is very interesting area to explore[21].

Bioprinting for cardiac tissue engineering: Cardiomyocytes (CMs) are the contractile cells of the heart. When stressed, cardiomyocytes undergo enlargement (hypertrophic growth) and apoptotic responses due to increased contractile force, which can lead to heart failure, both in vivo and in vitro cell culture models[22]. They are terminally differentiated cells that are extremely difficult to expand in vitro and are not able to compensate cell loss that occurs during myocardial infarction or chronic heart failure[23]. Most therapies used in clinical trials for cardiac tissue damage repair include cell replacement through application of bone marrow mesenchymal stem cells (MSCs), peripheral blood mononuclear cells or resident cardiac cells. However, their inability to proliferate and produce enough CMs limits the improvement or regeneration of damaged tissue. As an alternative, the combination of these cells with biomaterials such as bioprinting has emerged[24].

Proposed Research Strategy: ECM-based biomaterials have come up as great scaffold alternatives for tissue engineering, due to its important source of biochemical and biomechanical signals that support cell differentiation and function, as well as approximation to physiological conditions. Due to the need for 'smart' materials in tissue engineering, functional features were introduced to dECM hydrogels by the addition of dopants, including conductive polymers, magnetic nanoparticles and piezoelectric particles. One potential application of these, could be cardiac tissue engineering. The immaturity of hiPSC-CMs severely limit their use in cardiac tissue engineering. Conductive hydrogels have the potential to improve the maturity of cardiac cells engineered in vitro, by promoting electrical stimulation of the scaffolds, resulting in potential vascularization and stem cell differentiation to form properly functioning cardiac tissues. The aim of this work was to develop and bioprint ECM-based bioinks to produce electroconductive scaffolds for tissue engineering, with particular interest in cardiomyocyte maturation.

MATERIALS AND METHODS

sisECM digestion and hydrogel/bioink preparation: Decellularized extracellular matrix was obtained from porcine small intestine submucosa (sisECM), kindly provided by collaborators at the University of Nottingham. After decellularization, the sisECM was stored at -20ºC until further use. Briefly, for the preparation of 10 mg/mL sisECM stock solution, 1g of sisECM was digested in a solution containing 1 mg/mL of pepsin from porcine gastric mucosa (≥2.500 units/mg protein, Sigma-Aldrich) in 100 mL of 0.01 N HCl and stirred for 48-72 hours at room temperature. Once the sisECM was fully digested, aliquots were prepared and stored in the freezer at -20ºC or kept at 4ºC for immediate use.

8 mg/mL was selected as the working sisECM concentration. For the gelation of the sisECM[25], stock solution of digested sisECM was mixed with a neutralization buffer (NB). NB was prepared by mixing 0.1 N NaOH (1/10 of the volume of stock solution), 10x Phosphate Buffer Solution (PBS) (pH=7.4; Sigma-Aldrich;1/9 of the volume of stock solution) and 1x PBS (pH=7.4; Sigma-Aldrich; making up the final volume). It was then placed at 37ºC for gelation to occur. When mixing the different components, the formation of air bubbles in the solution must be avoided, as they can affect the mechanical properties of the gels.

Preparation of gelatin support bath for FRESH extrusion bioprinting: For the preparation of the gelatin support bath, an already existing protocol was followed[26]. DI water was preheated at 40-45ºC. Porcine skin gelatin (Type A, Sigma-Aldrich), 4% w/v, and $CaCl_2$ (Honeywell), 0.16% w/v, were added to the warmed water, maintaining agitation until all gelatin was dissolved and solution was clear. The solution was then kept overnight at 4ºC to ensure complete gelation on the blender

(SilverCrest) for ease of operation. When ready for use, the jar was filled with approximately the same volume of a 0.16% $CaCl_2$ solution as gelatin and all was blended with pulses for 60-90s. The desired amount was then pipetted to falcon tubes and centrifuged for 2 min, at 4500 rpm. The supernatant, as well as any foam that formed was removed.

PEDOT:PSS concentration adjustments: To the 8 mg/mL dECM hydrogel, PEDOT:PSS (Clevios PH1000, stock solution 1%) was added, by mixing thoroughly with a pipette.

Hydrogel Characterization

- Water content assay: Hydrogels were prepared and casted on cylindrical molds with 1 cm height and 1 cm diameter, containing 500 µL of the sisECM, sisECM + 0.05% PEDOT:PSS and sisECM + 0.1% PEDOT:PSS solutions. At least three samples of each material were prepared. After incubation for 30 minutes at 37ºC, molds were removed, and wet weights of each hydrogel were recorded. Samples were then dried at 60ºC. After complete water removal, the samples were weighed. The water content was calculated following Equation 1, where *Wdry* is the weight after water removal and *Wwet* is weight of the hydrated structures.

$$\frac{W_{wet} - W_{dry}}{W_{wet}} * 100\% \quad (1)$$

- Stability Assay: Hydrogels were prepared and casted on cylindrical molds with 1 cm height and 1 cm diameter, containing 500 µL of the sisECM, sisECM + 0.05% PEDOT:PSS and sisECM + 0.1% PEDOT:PSS solutions, one replicate per bioink. After incubation they were stored with PBS at room temperature for over 30 days.

Electrical characterization

- Conductivity: Hydrogels were prepared and casted on cylindrical molds with 1 cm height and 1 cm diameter, containing 500 µL of the sisECM, sisECM + 0.01% PEDOT:PSS, sisECM + 0.05% PEDOT:PSS and sisECM + 0.1% PEDOT:PSS solutions, with three replicates per bioink. Resistance (ρ) was recorded using a Velleman DVM832 digital multimeter, with fixed distance of 0.5 cm between tips. The electrical conductivity (σ) is the inverse of the resistance and was calculated using Equation 2.

$$\sigma = \frac{1}{\rho} \quad (2)$$

- Four-probe method: sisECM, sisECM + 0.05% PEDOT:PSS and sisECM + 0.1% PEDOT:PSS bioinks were prepared and 150 µL volume per sample was deposited on glass sheets and left to completely dry for 10 days, with three replicates per bioink. After samples were dried, four strips of gold electrodes were deposited on top of the materials by physical vapour deposition using an Edwards Vacuum Coating System E306A, across the entire film and with equal distance from each other. Electrodes were put in direct contact with the gold stripes and measurements were taken. Resistance was calculated using Equation 3, where t is the sample thickness (measured using a Bruker's Dektak 3.21 Profilometer (Bruker, Billerica, MA, USA), l is the length of the sample (varied between 0.47-1.4 cm), and the gap is the distance between gold bands (fixed distances between 330-2000 mm) . The electrical conductivity was calculated using Equation 2.

$$\rho = \frac{R * t * l}{gap} \quad (3)$$

- Electrochemical Impedance Spectroscopy (EIS): Hydrogels were prepared and casted on cylindrical molds with 1 cm height and 1 cm diameter, containing 400 µL of the sisECM, sisECM + 0.05% PEDOT:PSS and sisECM + 0.1% PEDOT:PSS solutions and stored in DI water until measurement. Five replicates per bioink were prepared. EIS analysis was performed using a PalmSen4 potentiostat in a two-electrode configuration. Data analysis was done using PSTrace software from PalmSens. The frequencies applied ranged between 0.1Hz and 10 MHz and the number of frequencies applied was 71.

Bioink Characterization

- Rheology (oscillating time sweep): A rheometer (model MCR92, Anton Paar) equipped with a 1° cone plate with a diameter of 50 mm was used to characterize the rheological properties of the bioinks. 500 µL of prepolymer solutions were prepared, with three replicates per bioink, and were then pipetted onto the rheometer. Initial plate temperature was kept at 4 °C. Viscosity was then determined through an oscillating time sweep under an amplitude of 1% and frequency of 1 Hz, for 20 minutes at 37 ºC.

- Printability: Printability was evaluated after the printing of a square mesh, with L= 20 cm. Photographs of the strands each condition were taken using a Fischer magnifying lens, with 0.63x magnification, and measures were manually taken using the ImageJ software.

Cell Culture

- hiPSCs culture and passaging: A REBL-PAT hiPSC cell line derived from a skin punch biopsy from a male subject was used. hiPSCs were cultured on Matrigel-coated plates and incubated at 37ºC in a 5% CO_2 atmosphere. Cells were cultured on E8 culture media (Essential 8 (Lifetech Cat no. A1517001); ThermoFischer) and media was changed on a daily basis. For hiPSCs passaging, culture media was aspirated, and cells were washed in PBS. After this, cells were incubated in TryplE (TrypLE Select (Life Tech #12563-029); ThermoFischer) for 3 min at 37ºC. TryplE was aspirated and cells were carefully detached from the bottom of the plate using the E8 solution. The desired concentration of cells was then transferred to a fresh Matrigel-coated plate containing 1:1000 of Rock inhibitor (Y27632, Tocris). For cell maintenance, media was changed every 2 days.

- hiPSCs differentiation towards cardiomyocytes: Differentiation of hiPSCs into cardiomyocytes was induced when cell confluence reached 90%, as previously reported[27,28]. Cells were preconditioned using E8 media supplemented with 1:1000 ROCK inhibitor. Media was changed in the subsequent two days with E8 and approximately, 60 hours after the preconditioning process started, media was changed to Stem-Pro 34 SFM (1X) media (2% StemPro™-34 Nutrient Supplement + 1% L-Glutamine (Lifetech Cat no. 10639011)), supplemented with 1:10000 BMP4 (R&D Systems Cat no. 314-BP-010) and 1:100 Matrigel. On day 0 of differentiation, media was changed to Stem Pro 34, supplemented with 1:1000 BMP4 and 1.6:1000 activin A (Lifetech Cat no. PHC9561). On day 2, media was changed to RPMI/B27 minus insulin (RPMI base media with B27 (Ins-) Lifetech Cat No. A1895601), supplemented with 1:1000 KY02111 and 1:1000 XAV939. On day 4, media is changed to RPMI/B27 (with insulin), supplemented with 1:1000 KY02111 (R&D Systems Cat Nos. 4731) and 1:1000 XAV939 (R&D Systems Cat Nos. 3748). From days 6 to 13, media is changed every 2 days to RPMI/B27 media (RPMI base media with B27 Lifetech Cat No. 17504044). After media is changed twice a week with RPMI/B27 for cell maintenance. All the different types of media used contained 1% Penicillin-Streptomycin (5,000 U/mL; Cat No. 15070063; ThermoFischer).

Cardiomyocytes were dissociated 10 weeks after differentiation following an existing protocol[27,28]. A dissociation solution was prepared with 1:2 Collagenase II (200 U/ml) solution in Ca2+ free HBSS (Hanks' Balanced Salt Solution; ThermoFischer), 1:1000 HEPES ((4-(2-hydroxyethyl)-1-piperazineethanesulfonic acid)), 1:1000 ROCK inhibitor and 1:1000 30 mM BTS (N-Benzyl-p-toluenesulphonamide). Cells were washed twice with warm HBSS solution and dissociation solution was then added and incubated for 3 hours at 37ºC. After incubation, cell suspension was removed from the plates and transferred to a 50 mL falcon tube, followed by the addition of a blocking buffer (prepared with plain RPMI media and 1:500 Dnase). Falcon tube contents were centrifuged for 15 minutes at 100 G, and then cells were resuspended in suspending media, prepared with RPMI/B27 media, 1:10 FBS (Fetal Bovine Serum) and 1:100 ROCKi. Cells are then prepared to be counted and plated using a hemocytometer. Cells were prepared to be counted using a hemocytometer and then plated in a new plate.

- Mouse fibroblast culture: L929 mouse fibroblasts with passaging numbers 11-14 were used. Culture media consisted on complete DMEM media supplemented with 10% FBS and 1% antibiotic. This media was changed every 3-4 days. In this case, a Trypsin-EDTA solution was used for cell passaging by incubation for 7 minutes followed by centrifugation for 7 minutes at 1250 RPM. Supernatant was removed and disposed, and cell pellet was resuspended with 1 mL of media. Cells were then plated on a new flask to the desired concentration and/or used for bioprinting assays.

- Imaging of cells: All the bright-field and fluorescence images were taken using a Leica DMI3000B microscope, with 4x, 10x and 20x magnifications. At least 3 images were taken for each of the samples and analyzed using ImageJ software.

Materials preparation for bioprinting

- Bioink and gelatin sterilization for bioprinting: All materials, including tubes, pipette tips, needles and other support materials were sterilized on the laminar flow hood with UV light for 30 minutes prior to bioprinting. For bioinks preparation, PEDOT:PSS and neutralization buffer were filtered with 0,22 µm filter (Millex-GV Syringe Filter Unit). All bioinks were then prepared under sterilized conditions on the laminar flow hood. In the case of the gelatin support bath, after gelatin and $CaCl_2$ dissolution on heated sterilized water, the solution was filtered using a 0.45 µm filter (Millex-GV Syringe Filter Unit), on the laminar flow hood. The 0.16% $CaCl_2$ solution was filtered using a 0,22 µm filter (Millex-GV Syringe Filter Unit).

Viability assays

- Live/Dead Assay: For the staining of viable cells, a solution of 1:1000 in PBS of Calcein-AM (Sigma-Aldrich) was prepared. For dead cells, the solution consisted of 2:1000 in PBS of Ethidium-homodimer-1 (Sigma Aldrich). After media removal from the wells with the target cells, the prepared solution was added to each sample and left to incubate for 20-30 minutes. Culture plates were protected from direct light to prevent photobleaching events. For cell seeding assays, sisECM, sisECM+0.05% PEDOT:PSS and sisECM+0.1% PEDOT:PSS bioink solutions were added to a 96-well plate and incubated at 37ºC for 30 minutes until gelification was complete. To sterilise the hydrogels, a solution of 5% penicillin-streptomycin (Pen-Strep) in PBS was added and left overnight at 4ºC.

- Cardiomyocyte's immunostaining: Cells were fixed with a 4% paraformaldehyde (PFA) solution in PBS and left to react for 20 minutes. PFA was removed and wells were washed with PBS and stored at 4ºC with when immunostaining was not immediately proceeded. After cell fixation, cardiomyocytes were immunostained. The first step was permeabilization, by the addition of 0.1% Triton x100 in PBS for 8 min at room temperature. After washing with PBS, 4% FBS in PBS was added for 1 h at room temperature for the blocking of non-specific binding. After washing with PBS, 1:1000 anti-TNNI3 (primary antibody, produced in mouse) in PBS was added and left overnight at 4ºC and washed with 0.05% Tween 20 in PBS. 1:1000 anti-mouse FITC in PBS was added for 1h at room temperature and washed with 0.05% Tween 20 in PBS. The nucleus was stained using Hoescht 5 µL/mL in PBS at 37ºC, followed by the washing with PBS. Finally, for actin staining, 1:150 phalloidin in PBS was added for 30 minutes at room temperature and washed with PBS.

Bioinks preparation for bioprinting

For cell bioprinting assays, 2 mL of each bioink was prepared and cell suspension media was added to each bioink at a concentration of $0.5x10^6$ cells/mL. Structures of circular geometry (r=2.5 mm) were printed.

RESULTS AND DISCUSSION

Optimization of bioinks composition

In the process of designing the bioinks, several PEDOT:PSS concentrations were tested according to results found in previous published studies[29-33]. It is important to note that the protocol that was followed to produce the sisECM hydrogels only works for final sisECM concentrations ranging from 6 to 8 mg/mL, as bellow 6 mg/mL gelation of the hydrogel did not allow for the self-support of the structures, leading to their collapse. All hydrogels were evaluated based on an arbitrary scale taking into account three parameters: circularity (this was the shape of the mould), PEDOT:PSS dispersion (related to the homogeneity of the PEDOT:PSS aggregates on the hydrogels, because the polymer chains are too big and due to the use of a simple mixing method that doesn't allow for perfect incorporation of the PEDOT:PSS in the sisECM) and the gelation outcome (formation of self-sustaining gel after incubation for 30 minutes at 37ºC and removal of the cast - for a complete gelation, sisECM concentration must be above 7 mg/mL). For this study, two conditions were selected, sisECM + 0.05% PEDOT:PSS (B) and sisECM + 0.1% PEDOT:PSS (C). A control condition, sisECM, is also analyzed and compared with PEDOT:PSS hydrogels (Figure 1).

Figure 1 - Casted hydrogels for sisECM (left), sisECM+0.05%PEDOT:PSS (center) and sisECM+0.1%PEDOT:PSS (right); incubation for 30 minutes at 37ºC.

Hydrogel Characterization

- Water content: A high water-content is important in a hydrogel so that it better represents the *in vivo* natural environments (~70%)[166]. As expected, the higher the PEDOT:PSS concentration on the bioink, the lower the water content is on the respective hydrogel. However, even for the sisECM + 0.1% PEDOT:SS condition, water content is considerably high, mimicking more accurately the tissue microenvironment. The water content of sisECM, sisECM +

0.05% PEDOT:PSS and sisECM + 0.1% PEDOT:PSS corresponded to 98.10 ± 0.10%, 98.04 ± 0.04% and 97.25 ± 0.04%, respectively.

- Stability of the casted structures: Hydrogel stability was evaluated though a period of 30 days. For this, casted hydrogels of all bioinks were stored at room temperature with PBS. During this time period, no observable deterioration of the structures was noticed, Figure 2, as confirmed by the calculation of their circularities where variations are negligible, making these hydrogels suitable for long term cell culture.

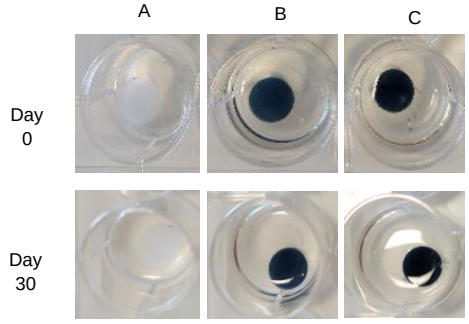

Figure 2 - Stability assay results for days 0 and 30 for all bioinks; A: sisECM; B:sisECM + 0.05% PEDOT:PSS; C: sisECM + 0.1% PEDOT:PSS.

- Four-probe Method: Conductivity values corresponded to $7.87x10^{-5}$ ± $1.72x10^{-6}$ S/m, $1.15x10^{-3}$ ± $6.96x10^{-4}$ S/m, $1.25x10^{-2}$ ± $2.85x10^{-3}$ S/m for sisECM, sisECM + 0.05% PEDOT:PSS and sisECM + 0.1% PEDOT:PSS, respectively. As expected, conductivity of the materials increases with higher PEDOT:PSS concentrations. It is important to note however, that this assay is not the most accurate since it was performed on dry samples, rather than wet samples that are closer to the real conditions, where a combination of electronic and ionic currents is taking place. This values, when compared to pure PEDOT:PSS (0.2-0.5 S/cm; 28 S/cm (wet) and 155 S/cm (dry)) or other conductive polymers (PANi: 0.1-0.2 S/cm; PPy: 0.02 S/cm) are within the range of values already recorded on previous works[34].

- Preliminary conductivity assay: Electrical characterization of wet samples is more accurate, as this represents the whole complexity of the hydrogel microenvironment. A preliminary conductivity assay was performed on wet hydrogels, by using a multimeter with a fixed distance between tips (0.5 cm). The higher the PEDOT:PSS concentration on the hydrogel, the higher the conductivity. We could also observe that even the lowest PEDOT:PSS concentration of 0.01% possesses a quantifiable conductivity. The values corresponded to $1.67x10^{-3}$ ± $7.33x10^{-5}$ S/m, $2.36x10^{-3}$ ± $2.46x10^{-4}$ S/m, $6.29x10^{-3}$ ± $1.30x10^{-3}$ S/m for sisECM + 0.01% PEDOT:PSS, sisECM + 0.05% PEDOT:PSS and sisECM + 0.1% PEDOT:PSS, respectively. Electrical conductivity is lower for dry samples due to the water content on wet samples, where water undergoes self-ionization that generates constant ionic flow on the hydrogels.

- Electrochemical Impedance Spectroscopy: EIS (Figure 3) was performed to measure the electrical impedance of the hydrogels over frequencies between 0.1 Hz and 10 MHz. Besides the hydrogels, impedance of copper bands was also measured as a positive control for total passage of electrical current. As expected, the higher the PEDOT:PSS concentration on the hydrogels, the lower the impedance to the passage of current. Impedances on the lower frequency range (until approximately 1000 Hz) usually correspond to the capacitive behaviour of the hydrogel and diffusion natural processes occurring within the biomaterial[35,36]. Electrochemical capacitors are electrochemical devices with fast and highly reversible charge-storage and discharge capabilities and are important for energy storage devices. PEDOT:PSS presence causes a shift in the measured impedance for hydrogels where the polymer is present. However, for higher frequencies, impedance of all hydrogels converges towards a stable value (that is higher with increasing PEDOT:PSS concentrations), meaning that it no longer has the capacity to accumulate charge and all electrical current passes through and behave like resistors (materials that oppose to the passage of current).

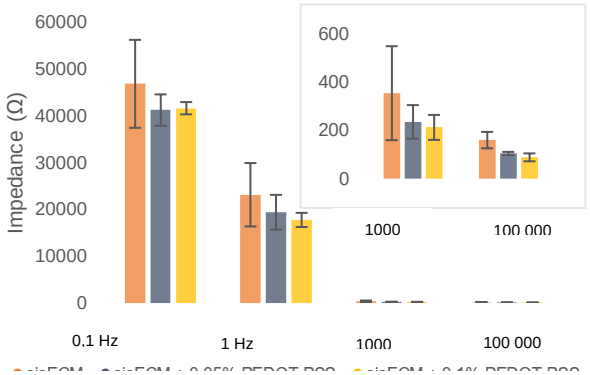

Figure 3 - Impedances for frequencies 0.1; 1; 1000 and 100000 Hz for sisECM, sisECM + 0.05% PEDOT:PSS and sisECM + 0.1% PEDOT:PSS hydrogels.

Optimization of the bioprinting conditions

- Rheological Characterization of the bioinks: A rheological analysis was performed through an oscillating time sweep assay to evaluate the bioink properties, including storage and loss modulus, G' and G'' respectively, loss factor (tan δ) and viscosity, η. It was observed that the storage modulus (elastic/solid state portion of the viscoelastic behavior) is higher than the loss modulus (viscous/liquid-state portion of the viscoelastic behavior), meaning that the transition from a solution to a gel was completed. Also, the higher the PEDOT:PSS concentration, the higher the initial and final values for both moduli (Figure 4). The gel point can be defined as the time at which the system loses fluidity and increases in viscosity and the fluid becomes solid like. It can be determined by the intersection of storage and loss modulus' curves. We could observe that in bioinks containing PEDOT:PSS the gelation process was faster than in plain sisECM bioink, where the gelation point corresponds to 0.833 minutes. For the other two bioinks, the gelation point happened before the measurement that was taking place, indicating that the gelation started almost immediately after the addition of the different elements of the bioink at 4ºC. This is theorized to happen due to mixing of PEDOT:PSS on the bioinks, that due to the low volume prepared increases temperature that contributes to gelation. Also, PEDOT:PSS might bond immediately with the ECM, promoting polymerization.

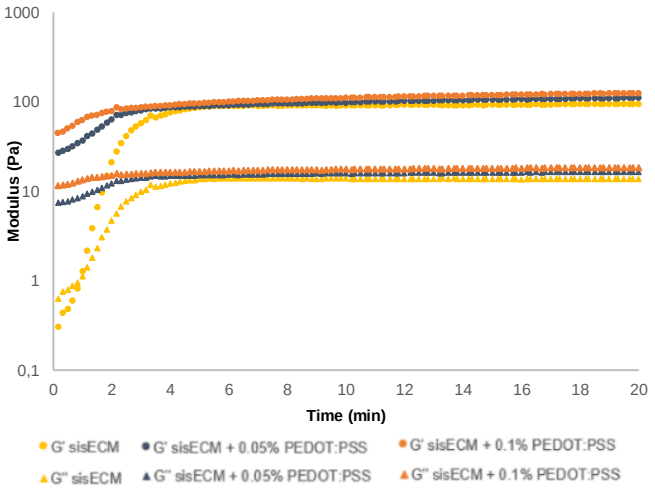

Figure 4 - Oscillating time sweep results for all bioinks; Variation of storage and loss modulus through time; $p < 0.05$ for Student's t-test

Loss factor (tan δ) and complex viscosity were also obtained. Loss factor relates to the energy dissipated during the sol-gel conversion and gives us information about the relation between potential energy and kinetic energy. It can be calculated by the ratio between loss modulus G'', that characterizes the deformation energy lost through internal friction when flowing, and the storage modulus G', that represents the stored deformation energy. As expected, at time point 0 and until 2 minutes, the sisECM bioink portraits a tan δ higher than the bioinks with PEDOT:PSS. This result indicates that the material behaves more liquid-like (as validated by previous results) and that the higher the PEDOT:PSS concentration, the lower the initial loss modulus, meaning that the sample is closer to a gel than a fluid (confirmed by gel point results). After complete gelation of all bioinks, tan δ stabilizes towards the same value. An analysis of the complex viscosity of the bioinks is important in bioprinting, as excessive viscosity values are directly related to a higher shear stress that could cause some harm to cells and reduce their viability values. Complex viscosity is a measure of the total resistance to flow as a function of angular frequency. The initial viscosity values stabilized after 5.67 minutes in sisECM, 3.5 minutes in sisECM + 0.05% PEDOT:PSS and 4.0 minutes in sisECM + 0.1% PEDOT:PSS. The average values obtained for complex viscosity range from 2.5-15 Pa.s, and so the values obtained are acceptable in bioprinting and should not cause a shear stress that would compromise the viability of the bioprinted cells.

- Tuning of bioprinting parameters: When printing there are some parameters that need to be considered and adjusted for optimal printing conditions that include: needle diameter to control resolution and levels of stress that cells might endure during the printing process; printing speed and dispensing pressure to control the amount of material being extruded (high pressures and low printing speeds cause too much material to be extruded limiting the final structure resolution); distance between layers to guarantee a compact structure (higher distance between layers can produce a structure that is not connected, and low distance between layers can cause an overlap between layers, leading to a deformed structure); number of layers to make sure that the printing structure is self-standing but does not collapse; and temperature to prevent gelation before printing. First of all, simple structures were printed to understand the printability conditions of the bioinks. The selection of the preliminary parameters was based on previous works[37-40] . It was observed that the higher the PEDOT:PSS concentration on the bioink, the higher the dispensing pressure during the printing process. This is due to the inability to perfectly homogenize and disperse the PEDOT:PSS on the bioink, and so some clogging happened, leading to the use of higher pressures. Also, as verified with rheology assays, viscosity increased with the addition of PEDOT:PSS, leading to increased dispensing pressures. For bioinks gelification and gelatin removal, the printed structures were incubated at 37ºC until gelatin was completely melted. Then, liquid gelatin was removed, and PBS solution was added to keep the printed structures hydrated during storage. However, despite the printing process being successful, the removal of the gelatin caused some damage to the structures due to the fragility of the sisECM hydrogels. Because of this, several changes were introduced.

First, all the plasticware required (needles, tubes, petri dish) was kept in the freezer at -20ºC until immediately before printing to prevent gelation of the bioinks due to a lack of temperature control on the bioprinter. All reagents used, including the gelatin, sisECM, neutralization buffer and $CaCl_2$ solution were also kept at 4ºC until immediately prior to use. Then, after printing, a 1% $CaCl_2$ solution was added on top of the gelatin to aid with the crosslinking of the sisECM hydrogel, as calcium is important in the assembly of ECM and binds to many ECM proteins, including laminin, fibrillin and collagen. During the melting process of the gelatin, the printed structures were placed in the incubator at 37ºC instead of the heating plate, to ensure homogeneous melting of the gelatin and complete polymerization of the hydrogel. Finally, PBS was added simultaneously to the removal of the liquified gelatin, to avoid overstretching the structures that could compromise their structural integrity. For the printing of the structures, instead of using a needle with 0.3 mm diameter, a 100 mL pipette tip was used, with a diameter of 0.57 mm. This improved the robustness of the printed constructs, especially for the bioinks with PEDOT:PSS, because aggregates of PEDOT:PSS were clogging the needle and compromising the printing process, and consequently the dispensing pressures lowered, and printing speeds increased. Also, because the corners of the structures were more prone to damage, structures with circular geometry were printed. Finally, distance between layers was also decreased, from 0.05 mm to 0.02 mm.

Evaluation of the printability

- Uniformity factor: The uniformity factor (U) was used to determine the uniformity between the printed strands and a theoretical perfectly uniform strand, Equation 4, were non-unifor strands have U>1. For comparison, printed structures only had one layer. Each bioink was printed at 25 mm/s printing speed and 0.1 psi extruding pressure. The measurements were taken before the gelatine removal to avoid the deformation of the structures when gelatine in removed. As seen in Figure 5A, no structures are completely uniform, where the uniformity factor got closer to 1 with

increasing PEDOT:PSS content. This can be expected as the high-water content and low viscosity of the materials leads to a loss in printing resolution in all cases and consequently does not allow for the maintenance of form and the ink disperses in the gelatin.

$$U = \frac{length\ of\ printed\ strand}{length\ of\ \ straight\ strand} \quad (4)$$

- Pore factor: The pore factor (Pr) was used to compare the printed structures to the CAD designs and how well they matched, Equation 5. For comparison, printed structures only had one layer. Each bioink was printed at 25 mm/s printing speed and 0.1 psi extruding pressure. Due to bioink dispersion on the gelatin, it is visible some deformity of the squares, with some pores even resembling a circular geometry rather than a square one (Figure 5B). Under-gelated bioinks will have a Pr<1, properly gelated bioinks will have Pr=1 and over-gelated bioinks will have a Pr>1. Contrary to what is expected to happen, the lower the PEDOT:PSS concentration on the bioink the closer the Pr is to 1, though this variation is not very noticeable. However, the higher the PEDOT:PSS concentration is in the bioink, more particles are present in the bioink and the more difficult it is to print, resulting in a more irregularly consistent final printed structure. As observed in Figure 5B, for sisECM the pores are mostly equal – also verified by the results for area and perimeter of each pore – whereas for sisECM+0.1% PEDOT:PSS not all pores are equal – area and perimeter of pores on the left of the mesh vary substantially form those on the right of the mesh, for example. Therefore, variability and deformity of the square pore is greater in the sisECM+0.1% PEDOT:PSS bioink.

$$Pr = \frac{(pore\ perimeter)^2}{16 * pore\ area} \quad (5)$$

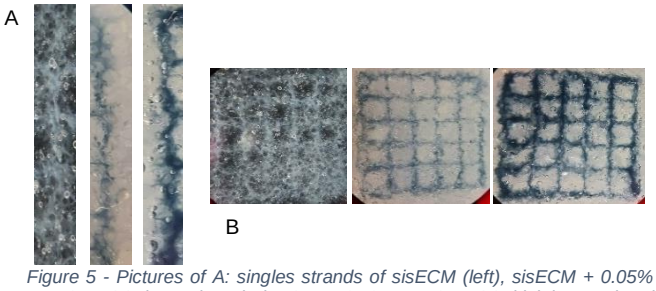

Figure 5 - Pictures of A: singles strands of sisECM (left), sisECM + 0.05% PEDOT:PSS (center) and sisECM + 0.1% PEDOT:PSS (right); B: printed square meshes of sisECM (left), sisECM + 0.05% PEDOT:PSS (center) and sisECM + 0.1% PEDOT:PSS (right)

- Wall thickness and Pore size: Wall thickness and pore diameter were also determined for each printed structure and compared to the dimensions of the original design. The printed structures used were the same as the ones used for pore factor determination. The results show that the higher the PEDOT:PSS concentration, the lower the wall thickness is and the higher the pore diameter is. These results are in accordance with what was expected, because the higher the PEDOT:PSS concentration, the higher the viscosity and the less the bioink disperses in the gelatin, and so there is less variation to the intended dimensions, with wall thickness of 0.57 mm and pore diameter of 16 mm.

Preliminary cell viability studies on the different hydrogel materials

In this part of the work, the main goal was to establish the scaffolds as viable platforms for cell proliferation and maintenance. For that purpose, proof-of-concept studies were performed using mouse fibroblasts. Once the viability of the fibroblasts was confirmed, this was also performed on hiPSC-CMs.

- Mouse fibroblasts: Initially, these cells were selected as they are frequently used in cytotoxicity evaluations, and they can be easily cultured and grown. L929 mouse fibroblasts were seeded on the different hydrogels to discard any cytotoxic effects derived from the materials. Cells cultured on a control material (96-well plate) were used as a positive control. Hydrogels were casted in 96-wells and incubated to induce their gelation. 10 000 cells were seeded per well for all conditions and at least 5 wells per condition were used. After cells were seeded on the different materials, their growth was followed throughout a week. On day 0, cells cultured on all conditions exhibited a rounded morphology, a characteristic of Trypsin-EDTA action for cell detachment. For cells cultured on the control material, from day 1 onwards the cells take a fusiform and spindle-shape typical of fibroblasts. The same morphology is observed for cells cultured on sisECM and sisECM + 0.05% PEDOT:PSS from day 3 onwards. However, for cells cultured on sisECM + 0.1% PEDOT:PSS hydrogels, cells always maintain a circular morphology. The round shape is a characteristic of the early stages of cellular adhesion but this morphology at longer time is associated with low attachment of cells to the surface. Also, for all conditions, cell division started on day 1 of cell culture. In all cases, the cell number increased after 7 days of culture, however this increase was more pronounced in the sisECM, where the final values in cell numbers were similar to the controls corresponding to 412 and 392, respectively, Figure 6. It is to note that from day 3 until day 7, the number of cells for the control condition plateaus because cells reached full confluence and there was no more space for cells to grow. In the materials containing PEDOT:PSS, the growth of cells was more limited. This is hypothesised to be caused by the lower cell adhesion on the conditions were PEDOT:PSS was present. Also, for conditions with PEDOT:PSS, the cells that adhered to the hydrogel did so in the sisECM part of the hydrogel, staying away from the PEDOT:PSS aggregates (the higher the PEDOT:PSS content, the lower the cell growth). This coupled with the limitation of only being able to capture some

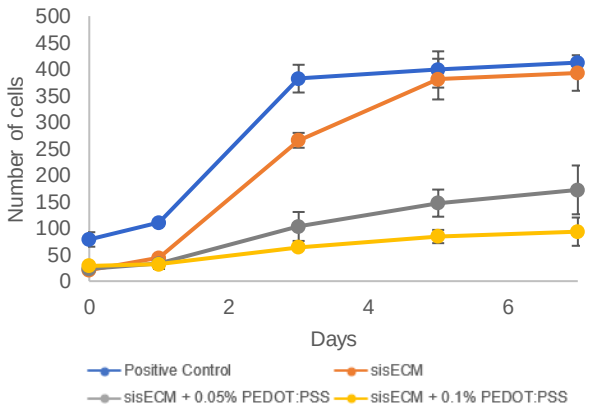

Figure 6 – Growth curve for cell viability assays for mouse fibroblasts, culture for 7 days, for cell seeding in sisECM, sisECM + 0.05% PEDOT:PSS and sisECM + 0.1% PEDOT:PSS hydrogels.

Cell viability was also analysed with a LIVE/DEAD assay on day 7, Figure 7. The results for sisECM, sisECM + 0.05% PEDOT:PSS and sisECM + 0.1% PEDOT: are 96.7±0.39%, 98.1±0.42% and 98.7±0.21%, respectively. For the positive control, cell viability is 99.40±0.09%. As observed, the higher the PEDOT:PSS concentration, the higher the cell viability. This is theorized to happen due to high cell number in the sisECM hydrogels (from days 1 to 7) when compared to PEDOT:PSS hydrogels, where cell confluence and limited nutrients might have led to cell death by the end of the 7 days. However, viabilities in all conditions are very high, confirming that not only do the scaffolds allow for cell proliferation, but also cell maintenance.

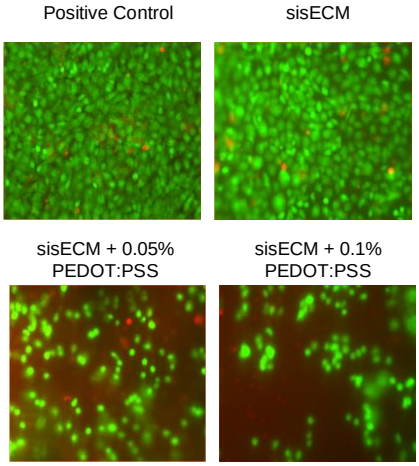

Figure 7 - Pictures taken with Leica fluorescence microscope (20x magnification) of fibroblasts seeded on the 3 different hydrogels and positive control on day 7 of cell culture. Green cells (alive) are stained with calcein-AM red cells (dead) with ethidium homodimer-1

- hiPSC-CMs: After establishing that the hydrogels are suitable for cell viability, experiments with cardiomyocytes were performed. Cardiac cells were used in this study because of the potential of this material in cardiac tissue engineering, not only due to the hydrogels' suitable electrical conductivity and mechanical stiffness, but also because of their similarity to natural tissue biological and chemical properties. The purity of the cardiomyocyte differentiation, meaning the % of cells on the plate that were actually cardiomyocytes (fibroblasts can easily be differentiated from hiPSCs) was calculated, and a value of 86±3% of cardiomyocyte purity was achieved, Figure 8.

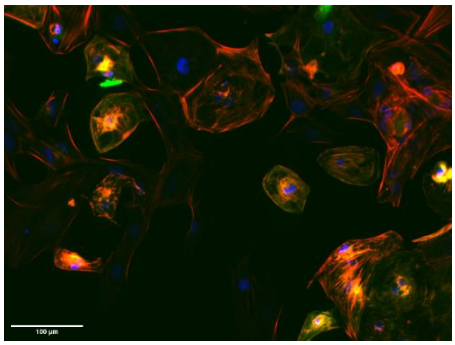

Figure 8 – Cardiomyocytes from the first differentiation batch. Photo taken with Leica microscope, at x10 magnification.

Once we have confirmed the success of the differentiation protocol, hiPSC-CMs were seeded on the different materials as we have previously done with the fibroblasts. In this case, the main difference between both cell types is that cardiac cells are non-proliferative cells and growth curves cannot be elaborated. For this reason, an immunostaining assay was carried out to determine the expression of cardiac-specific proteins. Immunostaining of these cells was performed using different fluorescence markers to identify the intracellular structures: cell nuclei (blue, Hoechst 33258), cytoskeleton actin fibres (red, Alexa Fluor-phalloidin) and cardiac sarcomeres (green, anti-TNNI3 specific antibody), Figure 9. It can be concluded that, due to the high purity of the differentiation of hiPSCs into cardiomyocytes, most of the cells are cardiomyocytes. The main conclusion that can be drawn from this assay is that cell density is higher on the positive control condition and decreases in the hydrogels, especially with the addition of PEDOT:PSS – decreasing amount of nucleus - as previously seen with fibroblasts cell seeding. This might be happening due to a lower cell adhesion of the cells on the hydrogels, especially those with PEDOT:PSS. Also, the higher the PEDOT:PSS content, the more aggregates it forms and, similarly to what was observed for fibroblasts, the less space it has for cardiomyocytes to adhere, as it looks like cells don't seed directly on top of a PEDOT:PSS aggregate. These cardiomyocytes present a rounder morphology, and a significantly lower size.

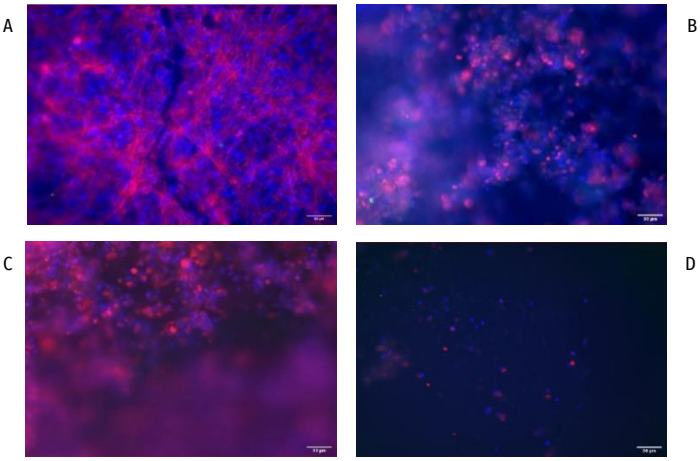

Figure 9 - Cardiomyocyte immunostaining results, on two different regions of the well plate; A: positive control; B: sisECM; C: sisECM + 0.05% PEDOT:PSS; D: sisECM + 0.1% PEDOT:PSS

Cell bioprinting

Once it was determined that cells could grow on the different materials, we proceeded with the bioprinting experiments. For this, the cells were added to the previously prepared bioinks.

- Mouse Fibroblasts: Firstly, 2 mL of each bioink was prepared, to which 200 µL of cell suspension media was added at a concentration of $0.5x10^6$ cells/mL. In accordance with the optimal printing conditions previously determined, structures of circular geometry (r=2.5 mm) were printed, Figure 10. On day 0, pictures of the printed structures were taken before and after gelatin removal. Their structural maintenance was not achieved mainly due to the decreased concentration of sisECM on the final hydrogel as it lowered with the addition of the cells suspension. Also, it was not possible to control the temperature as accurately as before since the materials were sterilized it was not possible to keep needles and tubes at 4ºC. This triggered gelation before the materials were extruded, causing some clogging in the needle tip and limiting the printability of the materials. After gelatin removal, the printed structures were left in the

incubator at 37ºC with DMEM-media, replaced every 2 days. Until day 3, for PEDOT:PSS hydrogels conditions, cells exhibited a small and round morphology, whereas for the sisECM hydrogels, from day 1 onwards, cells presented a spindle shape morphology. From day 5 onwards, cells in sisECM+0.05% PEDOT:PSS exhibited also presented a spindle shape morphology, and cells cultured on sisECM + 0.1%PEDOT:PSS hydrogels still presented a round morphology (in accordance with cell seeding results). This means that cell adherence might take longer to occur on printed hydrogels.

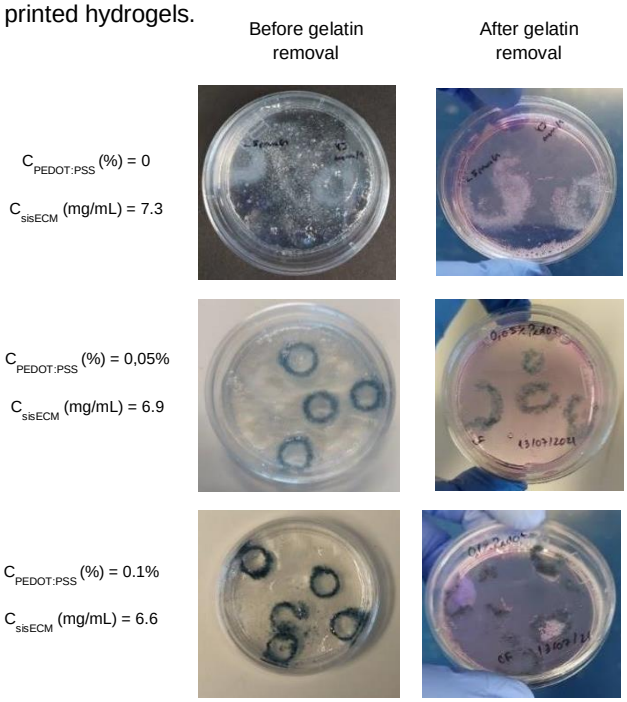

Figure 10 - Photos of printed structures taken before and after gelatin removal on day 0; printing speed of 45 mm/s, dispensing pressure of 0.1psi, 3 layers and 0.05 mm between layers for all conditions

As expected, cell viability is higher in the cell seeding assay, although cell viability for printed structures is > 95%. For sisECM, sisECM + 0.05% PEDOT:PSS and sisECM + 0.1% PEDOT:PSS cell viabilities are of 95.21±1.0%, 95.09±1.3% and 98.72±1.7%, respectively. This difference can be explained by the exposure of the cells to the printing process. It is important to note that cells undergo mixing with the bioink, that even though was a gentle mixing, it was not possible to guarantee integrity of all cells. Also, the bioinks were kept at 4ºC, meaning that cells were exposed to thermic shock, which might have also impacted cell integrity during the printing process.

To solve the problem of structural integrity not being maintained after gelatin removal, an adjustment in sisECM concentration was performed, where sisECM was kept at 8.0 mg/mL in the final bioink preparation after addition of 200 µL of cell suspension at a concentration of 0.5x106 cells/mL. Also, the number of layers of the printed structure was increased from 3 to 5. On day 0, pictures of the printed structures were taken before and after gelatin removal. Their structural maintenance was achieved, with exception of some constructs of sisECM + PEDOT:PSS conditions due to inconsistencies in the printing process, related to clogging of the needle due to the formation of PEDOT:PSS aggregates, causing some of some of the layers to not be properly printed. The structural integrity was also maintained after 7 days of cell culture at 37ºC, with media changes every two days.

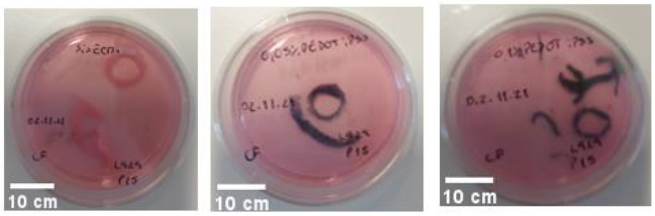

Figure 11 - Photos of printed structures taken on day 7; printing speed of 45 mm/s, dispensing pressure of 0.1psi, 5 layers and 0.05 mm between layers for all conditions; from left to right: sisECM, sisECM+0.05%PEDOT:PSS and sisECM+0.1%PEDOT:PSS, respectively.

Alternative Bioinks

- Alginate-gelatine conductive bioink: An alginate + gelatin (alg-gel) hydrogel was prepared to evaluate and compare to the conductive properties and biocompatibility of the sisECM bioinks. The formulation of this ink was based on previous works[41] and consisted of alg-gel solution with 1:1 proportion of 5% alginate and 15% gelatin was prepared, resulting in an 2.5%-7.5% alg-gel bioink. On top of the mold, 0.16% $CaCl_2$ was added to allow for alginate crosslinking, and the structures were left to gelate at room temperature for 20 minutes. After this, the casts were removed. However, despite successful hydrogel preparation and bioprinting, a lack of mechanical stability – after 3 days in PBS + 0.04%CaCl2 solution, structures started collapsing until total dissolution for all PEDOT:PSS concentrations – no more experiments were performed.

- Magnetic field-responsive hydrogels: Besides electrical stimulation, magnetic stimulation has also been reported to improve cardiomyocyte maturation. The magnetic properties were introduced by the addition of non-functionalized iron oxide (Fe_3O_4) nanoparticles. These nanoparticles have been shown, in combination with hydrogels, to be able to respond to a variation in magnetic field on a fast mode, with reversible changes of their shape and volume. In the process of designing the bioinks, several Fe_3O_4 nanoparticles concentrations were tested, based on the already used concentrations for the previously formulated sisECM-PEDOT:PSS hydrogels. For the magnetic particles' hydrogels, sisECM concentration was maintained at 8 mg/mL, and the Fe_3O_4 particles diluted in neutralization buffer. After preparation, the bioinks were casted in the previously used molds and incubated at 37ºC, with varying incubation times depending on the particle's concentration. sisECM + 0.2% Fe_3O_4 was the formulation chosen for further testing, as this bioink achieved optimal marks according to the scale set up for circularity, particles' dispersion and gelation. A contact angle assay was performed, and results for sisECM + 0.2% Fe_3O_4 are of 24.15±2.47º and 12.13±2.20º for 0T and 0.08T, respectively. This indicates that in the presence of a magnetic field, the contact angle lowers, making the material more wetting (the closer to 0º the more spreading of the liquid; the closer to 180º, the more non-wetting the material is).

CONCLUSIONS AND FUTURE REMARKS

This work was successful in developing a novel ECM-based conductive bioink for FRESH-extrusion based bioprinting of

biocompatible scaffolds for potential application in cardiac tissue engineering. Electrochemical characterization of these scaffolds allowed the establishement of PEDOT:PSS hydrogels as viable electroconductive polymer-based scaffolds, with conductivity values in accordance to those found in literature, behaving as a capacitator at low frequencies and a resistor at high frequencies (>10000 Hz) regardless of PEDOT:PSS concentration. The capacitive behavior is attractive for potential application as energy storage devices. The scaffolds produced are not only stable for long-term cell culture, but also have suitable rheological and printability properties adequate for FRESH-extrusion bioprinting, though mechanical stability and shape-fidelity were hindered by the limitation of temperature control, due to early polymerization of the sisECM with the addition of PEDOT:PSS. Proof-of-concept cell-based experiments allowed the verification of the bioink compatibility with both mouse fibroblasts and hiPSC-CMs. Regarding cell bioprinting, sisECM concentration adjustment needs to be done to improve bioprinted constrcuts mechanical stability. Also, the bioprinting of cardiomyocytes and eletrical stimulation on these sisECM - PEDOT:PSS bioprinted scaffolds can be done to evaluate if cardiomyocyte maturation is improved. Finally, sisECM-based bioinks have the potential to be altered for magnetic stimulation, with iron oxide magnetic particles, as demonstrated in this work, though further testing to investigate its biocompatibility and impact of magnetic-field exposure on cardiomyocyte maturation needs to be done. With this in mind, sisECM-based bioinks also have the potential to be formulated with piezoelectric nanoparticles for application in cardiac tissue engineering.

REFERENCES

1. Caddeo, S., Boffito, M. & Sartori, S. Tissue Engineering Approaches in the Design of Healthy and Pathological In Vitro Tissue Models. *Front. Bioeng. Biotechnol.* **0**, 40 (2017).
2. S, D. *et al.* 3D bioprinting for biomedical devices and tissue engineering: A review of recent trends and advances. *Bioact. Mater.* **3**, 144–156 (2018).
3. Askari, M. *et al.* Recent progress in extrusion 3D bioprinting of hydrogel biomaterials for tissue regeneration: a comprehensive review with focus on advanced fabrication techniques. *Biomater. Sci.* **9**, 535–573 (2021).
4. Jia, J. *et al.* Engineering alginate as bioink for bioprinting. *Acta Biomater.* **10**, 4323 (2014).
5. Phillippi, J. A. *et al.* Microenvironments Engineered by Inkjet Bioprinting Spatially Direct Adult Stem Cells Toward Muscle- and Bone-Like Subpopulations. *Stem Cells* **26**, 127–134 (2008).
6. FY, H., HH, L. & SH, H. 3D bioprinting of neural stem cell-laden thermoresponsive biodegradable polyurethane hydrogel and potential in central nervous system repair. *Biomaterials* **71**, 48–57 (2015).
7. Raman, R. & Bashir, R. Stereolithographic 3D Bioprinting for Biomedical Applications. *Essentials 3D Biofabrication Transl.* 89–121 (2015) doi:10.1016/B978-0-12-800972-7.00006-2.
8. JY, P. *et al.* A comparative study on collagen type I and hyaluronic acid dependent cell behavior for osteochondral tissue bioprinting. *Biofabrication* **6**, (2014).
9. R, G. *et al.* Patterning human stem cells and endothelial cells with laser printing for cardiac regeneration. *Biomaterials* **32**, 9218–9230 (2011).
10. Catros, S., Guillotin, B., Bačáková, M., Fricain, J. C. & Guillemot, F. Effect of laser energy, substrate film thickness and bioink viscosity on viability of endothelial cells printed by laser-assisted bioprinting. *Appl. Surf. Sci.* **257**, 5142–5147 (2011).
11. Wang, Z. *et al.* A simple and high-resolution stereolithography-based 3D bioprinting system using visible light crosslinkable bioinks. *Biofabrication* **7**, 045009 (2015).
12. Murphy, S. V & Atala, A. 3D bioprinting of tissues and organs. *Nat. Biotechnol. 2014 328* **32**, 773–785 (2014)
13. Gao, T. *et al.* Optimization of gelatin–alginate composite bioink printability using rheological parameters: a systematic approach. *Biofabrication* **10**, 034106 (2018).
14. Hinton, T. J. *et al.* Three-dimensional printing of complex biological structures by freeform reversible embedding of suspended hydrogels. *Sci. Adv.* **1**, (2015).
15. Noor, N. *et al.* 3D Printing of Personalized Thick and Perfusable Cardiac Patches and Hearts. *Adv. Sci.* **6**, 1900344 (2019).
16. YJ, C. *et al.* A 3D cell printed muscle construct with tissue-derived bioink for the treatment of volumetric muscle loss. *Biomaterials* **206**, 160–169 (2019).
17. Verena Schwach & Robert Passier. Native cardiac environment and its impact on engineering cardiac tissue. *Biomater. Sci.* **7**, 3566–3580 (2019).
18. Shavandi, A. *Biomimetics*. (IntechOpen, 2021).
19. A, P. & LP, T. Current Status of Bioinks for Micro-Extrusion-Based 3D Bioprinting. *Molecules* **21**, (2016).
20. D, C., HW, T., T, W. & MW, N. Organ-Derived Decellularized Extracellular Matrix: A Game Changer for Bioink Manufacturing? *Trends Biotechnol.* **36**, 787–805 (2018).
21. Bhat, M. A., Rather, R. A. & Shalla, A. H. PEDOT and PEDOT:PSS conducting polymeric hydrogels: A report on their emerging applications. *Synth. Met.* **273**, 116709 (2021).
22. Woodcock, E. A. & Matkovich, S. J. Cardiomyocytes structure, function and associated pathologies. *Int. J. Biochem. Cell Biol.* **37**, 1746–1751 (2005).
23. Eschenhagen, T., Didié, M., Heubach, J., Ravens, U. & Zimmermann, W. H. Cardiac tissue engineering. *Transpl. Immunol.* **9**, 315–321 (2002).
24. Arnal-Pastor, M., Chachques, J. C., Pradas, M. M. & Vallés-Lluch, A. Biomaterials for Cardiac Tissue Engineering. (2013)
25. N, A., H, P., GR, K., KM, S. & LJ, W. Bone extracellular matrix hydrogel enhances osteogenic differentiation of C2C12 myoblasts and mouse primary calvarial cells. *J. Biomed. Mater. Res. B. Appl. Biomater.* **106**, 900–908 (2018).
26. Hinton, T. J. *et al.* Three-dimensional printing of complex biological structures by freeform reversible embedding of suspended hydrogels. *Sci. Adv.* **1**, (2015).
27. Vaithilingam, J. *et al.* Multifunctional Bioinstructive 3D Architectures to Modulate Cellular Behavior. *Adv. Funct. Mater.* **29**, 1902016 (2019).
28. Mosqueira, D. *et al.* CRISPR/Cas9 editing in human pluripotent stem cell-cardiomyocytes highlights arrhythmias, hypocontractility, and energy depletion as potential therapeutic targets for hypertrophic cardiomyopathy. *Eur. Heart J.* **39**, 3879–3892 (2018)
29. Spencer, A. R. *et al.* Bioprinting of a Cell-Laden Conductive Hydrogel Composite. *ACS Appl. Mater. Interfaces* **11**, 30518–30533 (2019).
30. Heo, D. N. *et al.* Development of 3D printable conductive hydrogel with crystallized PEDOT:PSS for neural tissue engineering. *Mater. Sci. Eng. C* **99**, 582–590 (2019).
31. Aggas, J. R., Abasi, S., Phipps, J. F., Podstawczyk, D. A. & Guiseppi-Elie, A. Microfabricated and 3-D printed electroconductive hydrogels of PEDOT:PSS and their application in bioelectronics. *Biosens. Bioelectron.* **168**, 112568 (2020).
32. Roshanbinfar, K. *et al.* Electroconductive Biohybrid Hydrogel for Enhanced Maturation and Beating Properties of Engineered Cardiac Tissues. *Adv. Funct. Mater.* **28**, 1803951 (2018).
33. Nyoung, H. *et al.* Directly Induced Neural Differentiation of Human Adipose-Derived Stem Cells Using Three-Dimensional Culture System of Conductive Microwell with Electrical Stimulation. *https://home.liebertpub.com/tea* **24**, 537–545 (2018).
34. Yuk, H. *et al.* 3D printing of conducting polymers. *Nat. Commun. 2020 111* **11**, 1–8 (2020).
35. Oldenburger, M. *et al.* Investigation of the low frequency Warburg impedance of Li-ion cells by frequency domain measurements. *J. Energy Storage* **21**, 272–280 (2019).
36. Nguyen, T. Q. & Breitkopf, C. Determination of Diffusion Coefficients Using Impedance Spectroscopy Data. *J. Electrochem. Soc.* **165**, E826 (2018).
37. W, L. *et al.* Extrusion Bioprinting of Shear-Thinning Gelatin Methacryloyl Bioinks. *Adv. Healthc. Mater.* **6**, (2017).
38. Adhikari, J. *et al.* Effects of Processing Parameters of 3D Bioprinting on the Cellular Activity of Bioinks. *Macromol. Biosci.* **21**, (2021).
39. Gillispie, G. J. *et al.* The Influence of Printing Parameters and Cell Density on Bioink Printing Outcomes. *https://home.liebertpub.com/tea* **26**, 1349–1358 (2020).
40. Colosi, C. *et al.* Microfluidic Bioprinting of Heterogeneous 3D Tissue Constructs Using Low-Viscosity Bioink. *Adv. Mater.* **28**, 677–684 (2016).